

Equilibrium-based simulation of lignocellulosic biomass pyrolysis via Aspen Plus[®]

ALESSANDRO VISCONTI¹, MICHELE MICCIO¹ and DAGMAR JUCHELKOVÁ²

¹Department of Industrial Engineering

University of Salerno

Via Giovanni Paolo II, 132 – 84084 Fisciano (SA)

ITALY

mmiccio@unisa.it http://www.diin.unisa.it/diin_en/index_en

²Faculty of Mechanical Engineering, Department of Energy

VŠB - Technical University of Ostrava

17. listopadu 15, Ostrava - Poruba

CZECH REPUBLIC

dagmar.juchelkova@vsb.cz <http://profil.vsb.cz/juh20>

Abstract: Among the several methods to upgrade biomasses to better fuels, pyrolysis is the one that is receiving more and more attention. Many authors have developed kinetic-based models that are quite accurate, but computationally intensive and applicable only to specific pyrolysis installations within certain operating conditions. This work has been focused on the development of an input-output model through the software Aspen Plus[®] that could simulate the equilibrium-based pyrolysis of a lignocellulosic biomass and, as a minimum, could predict the effects of the main process variables on the most relevant performance results. The most weighty assumption is that the thermodynamic equilibrium is achieved within the pyrolysis reactor. The trends of the predicted results as a function of the process operating variable are generally in accordance with those that are experimentally evident and published in literature. Vice versa, the Aspen code could not predict the composition of the liquid residue, i.e., tar.

Key-Words: Biomass – Pyrolysis – Aspen – Equilibrium – Gibbs free energy – Char - Tar

1 Introduction

Traditional biomass energy sources accounted for 10% of total energy consumption worldwide in 2009, being the predominant energy source for approximately 2.7 billion people facing energy scarcity [1]. Nowadays, technological as well as political objectives are those of extending their energy-related applications and making their use as efficient as possible: as a consequence, research is focusing more and more on them [2,3,4,5].

The biomass conversion processes can be grouped in three main categories: thermochemical, chemical and biochemical conversion. Among the thermochemical processes the most important ones are combustion, gasification, pyrolysis and, more recently, torrefaction. In the last two in the list, the leading factor is heat, which converts biomass into other substances. Pyrolysis is a modern thermochemical decomposition process at elevated temperatures in the absence of oxygen, that is, in an inert atmosphere. This process is now being used quite heavily in the chemical industry, for example, to produce methanol, activated carbon and char from wood or coke from coal; anyway, besides the solid residue called char also valuable gaseous and liquid products are obtained with pyrolysis. The gas

obtained contains mostly H₂, CO, CO₂, H₂O and CH₄, whereas the liquid, usually called tar, is a complex mixture of hydrocarbons. A simplified process scheme for biomass pyrolysis is in figure 1. The char is usually referred to as the mass of solid remaining after the pyrolysis, including both that coming from the reactor and that captured in the particle separator (figure 1), i.e., cyclone or filter. There is some confusion in literature about the meaning of the word “bio-oil”, for which it is possible to find different synonyms (tar, pyrolytic liquids, bio-crude, etc.). The most used definition of tar is that it refers to the whole liquid fraction, that is, organic compounds + pyrolytic water + feedstock moisture (e.g. [6]). Pyrolytic gas and carrier gas are obtained once the bio-oil is removed in the condensers (figure 1).

At the heart of a pyrolysis process there is the reactor. Although it probably represents only about 10-15% of the total capital cost of an integrated system, most of research and development has focused on testing and developing different reactors on a variety of feedstocks.

The most popular technological options for the pyrolysis reactor are the bubbling fluidized bed (BFB), the circulating fluidized bed (CFB), the

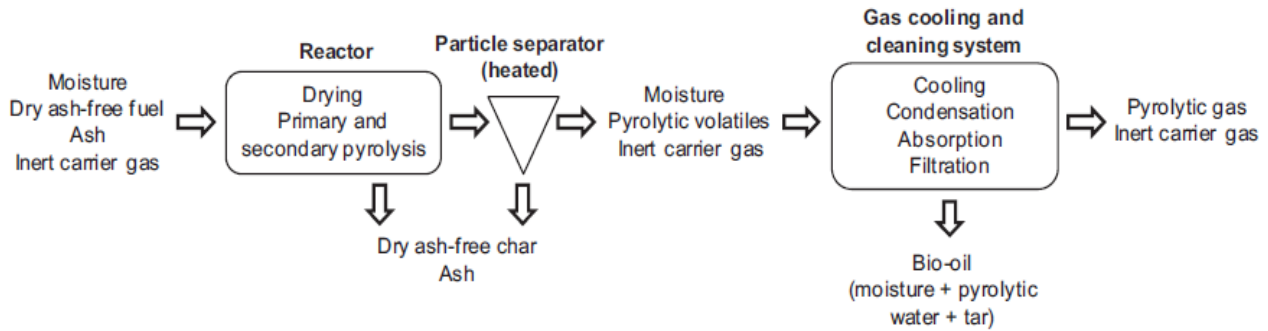


Fig. 1: simplified process scheme for biomass pyrolysis.

transported bed, the fixed bed (FB), the rotating cone [7], the ablative reactor [8], the screw and the auger reactors [9]. Some authors, looking at the results got with biomass gasification, have investigated also the effect of some common catalysts like the nickel-based ones [10].

Vegetative or lignocellulosic biomass, also known as phytomass, is composed primarily of cellulose, hemicellulose and lignin, along with lesser amounts of extractives (e.g., terpenes, tannins, fatty acids, oils and resins), moisture and mineral matter [11]. Several groups studied the pyrolysis of biomass on the basis of those three main components. Raveendram et al. [12] investigated the pyrolysis characteristics of biomass components in a thermogravimetric analyzer and a packed-bed pyrolyzer and found no detectable interactions among the components during pyrolysis in each experimental setup. Yang et al. [13] also observed negligible interactions among the three biomass components in their study, when using a thermogravimetric analyzer. On the other hand, Worasuwannarak et al. [14] studied the pyrolysis behavior of cellulose, xylan, lignin and mixtures by TG-MS technique and observed significant interactions between cellulose and lignin that caused a suppression of liquid product formation and an increase in the yield of solid residue. Wang et al. [15] also reported cellulose-lignin interactions, as well as hemicelluloses-lignin interactions, while they reported that hemicelluloses and lignin did not seem to affect each other during pyrolysis in a thermogravimetric analyzer. More recently, Wang et al. [16] studied the interactions of the biomass components in both a TG-FTIR and an experimental pyrolyzer. They reported no significant differences between the experimental and calculated TG/DTG curves, when using biomass component mixtures, but differences in the evolution curves of the main products (levoglucosan, 2-furfural, acetic acid and 2,6-dimethoxy phenol) were apparent. In addition,

the mixed samples exhibited a common tendency to form less liquid and more gas products than what the calculations predicted. So, although these studies did not prove the complete independence of these three main components on each other during thermal degradation, many authors studied the pyrolysis of hemicelluloses, cellulose and lignin individually and some of them proposed kinetic schemes as a compromise capable of describing satisfactorily the pyrolysis of a variety of biomasses [17,18,19,20,21,22].

2 Problem Formulation

Aspen Plus[®][23] is a comprehensive chemical process modelling system, used by both academy and industry, for design, simulation, process improvement and optimization. Aspen Plus[®][23] has advanced and dedicated functionalities, such as detailed heat exchanger design, dynamic simulation, batch process modelling. It also has a facility for using an equation-based approach in some of its routines, which permits convenient use of design specifications in process modelling.

In this work, the equilibrium-based simulation of the pyrolysis of a lignocellulosic biomass feedstock via Aspen Plus[®] has been attempted. Precisely, the description of pyrolysis follows a non-stoichiometric approach, that is, no particular reaction is specified. Apart from pyrolysis, a number of elementary steps are identified and represented as model blocks for simplified process simulation (figure 2).

These are the main assumptions on which this model is based:

- The blocks are implicitly considered to be zero-dimensional and are regarded as perfectly insulated (e.g., the heat losses are neglected).
- Perfect mixing and uniform temperature are assumed in each block

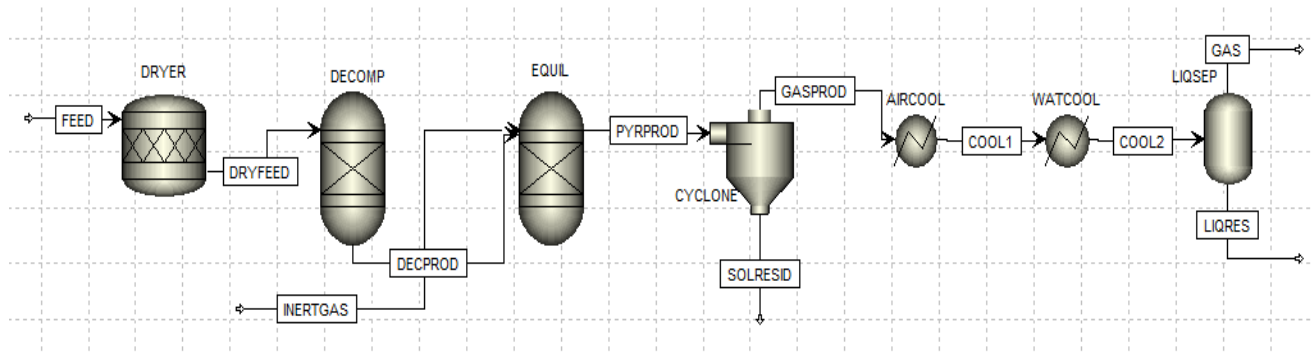


Fig. 2: flowsheet of the pyrolysis process implemented in Aspen Plus®.

- residence time is long enough to reach the thermodynamic equilibrium in the reaction blocks.
- reaction pathways and formation of intermediates are not taken into account.

The flowsheet of the model developed with Aspen Plus® is represented in figure 2.

The similarity is readily noticed with the simplified scheme of pyrolysis represented in figure 1. In fact, in both figures, the process can be divided in two sections: the first of pyrolysis/reaction and the second of separation/recovery.

The actual reaction section, in which drying, primary and secondary pyrolysis of feedstock take place, is modelled by the first three blocks, that is, the DRYER, the DECOMP and the EQUIL in figure 2. Actually, they are just three reactor blocks from the reactor library of Aspen Plus®.

The first block called DRYER is an “RStoic block”, takes as input the wet biomass, named FEED, and simulates the drying stage. This block requires that the amount of removed water (per unit mass of total feed, excluding inerts) must be specified.

The second block, called DECOMP, is an “RYield block” and takes as input the dried biomass, named DRYFEED. This block requires that the yields of the products (per unit mass of total feed, excluding any inert components) must be specified. DECOMP predicts the decomposition, at fixed temperature and pressure, of the feedstock into reference components that are: C (fixed carbon), ash, H₂O, H₂, Cl₂, S, O₂ and N₂.

For each of the blocks, i.e., DRYER and DECOMP, an external, user-supplied FORTRAN subroutine carries out the mass balance calculations and supplies the right input values as inputs.

The third block, which completes the pyrolysis section, is an “RGibbs block” named EQUIL. This block takes in input the decomposed biomass and the inert gas feed, named respectively DECPROD and INERTGAS. The RGibbs block uses Gibbs free

energy minimization with phase splitting to calculate thermodynamic equilibrium and it does not require reaction stoichiometry. The criteria for thermodynamic equilibrium affirm that an isothermal and isobaric chemical system is at equilibrium when the Gibbs free energy is minimized. The minimization is obtained by solving a nonlinear constrained problem using a penalty function method (SUMT) [24]. Within this simulation the EQUIL block takes as input the reference components coming from the DECOMP block and the inert gas and, by minimizing the Gibbs free energy, it calculates the simultaneous phase and chemical equilibrium at fixed temperature and pressure; as output, there are the species that have been specified in the EQUIL block as “possible products”.

The reference biomass feedstock here considered for simulation is the same tested in the pyrolysis experiments of Honus[25]. It comes from waste wood and forestry residues. Honus[25] fed it into the pyrolysis reactor in the form of pellets with particle sizes less than 20 mm. Table 1 shows the ultimate and proximate analysis of this biomass.

A necessary input to perform the simulation is also the sulfur analysis, by specifying the relative quantities of pyritic, sulfate and organic sulfur. Actually, it was not available in Honus[25]; therefore, it has been supposed that the sulfur within the biomass is equally distributed among these three species. Table 2 reports the sulfur distribution among the three sulfuric species.

Table 3 summarizes the reference processing conditions of the pyrolysis model.

The operating variables are pyrolysis temperature, pyrolysis pressure, oxygen content in the inert gas stream, inert gas flow rate, temperature of the inert gas stream, biomass feed rate and the feed chemical composition. Table 4 shows the values assigned to each operating variable.

Concerning gas properties, although the status of ideal gas could be chosen because of high temperature and low pressure, the Peng-Robinson

method has been preferred because it is based on a cubic equation of state, which can take in account possible non-ideal behaviors [26].

Ultimate analysis			
wt. % d. b.			
Component	Biomass	Tyres	Brown coal
C	47.67	85.4	63.51
H	6.86	7.56	5.14
N	0.13	0.48	1.01
Cl	0	0	0
S	0.01	0.44	0.06
O	43.98	0.01	24.58
Proximate analysis			
wt. % d. b.(except moisture)			
Component	Biomass	Tyres	Brown coal
Moisture	7.86	1.71	13.56
Volatiles	84.71	70.86	52.51
Fixed C	13.94	23.03	41.79
Ash	1.35	6.11	5.70

Table 1: ultimate and proximate analyzes of the sample of lignocellulosic biomass together with two reference fuels.

Sulfur analysis			
wt. % d. b.			
Component	Biomass	Tyres	Brown coal
Pyritic S	0.0033	0.14	0.02
Sulfate S	0.0033	0.14	0.02
Organic S	0.0034	0.16	0.02

Table2: sulfur distribution in the sample of lignocellulosic biomass together with two reference fuels.

Blocks	T (°C)	Pressure (bar)			Other inputs
DRYER	500	1			
DECOMP	500	1			
EQUIL	500	1			
CYCLONE	500	1			
AIRCOOL	300	1			
WATCOOL	40	1			
LIQSEP	40	1			
Streams	T (°C)	Pressure (bar)	Flow rate	Mole comp.	Other inputs
FEED	25	1	50 kg/h	See prox. and ult. analyses	Sizes up to 20 mm
INERTGAS	25	1	0.5 kg/min	99% N ₂ , 1% O ₂	-

Table 3: reference input data to the ASPEN® pyrolysis model.

For what concerns the results predicted by the simulation, the focus has been put on the most relevant ones, which are:

- relative mass quantities of char, tar and gas produced
- relative concentrations of CO, CO₂, H₂, CH₄ and H₂O in the pyrolysis gas
- carbon fraction in the pyrolyzed solids

- pollutant concentrations in the pyrolysis gas
- char higher heating value
- gas lower heating value
- net heat duty to the pyrolysis reactor

Characteristic computation times of the Aspen code are in the order of seconds on a PC with the Windows 8.1 operating system, i7 processor and 4 Gb RAM.

Operating variable	Range	Increment
Pyrolysis temperature	350-750 °C	50 °C
Pyrolysis pressure	1-10 bar	1 bar
Inert gas O ₂ content	1-9 % mole fraction	1 %
Inert gas flow rate	0.1-1 kg/min	0.1 kg/min
Feed flow rate	10-100 kg/h	10 kg/h
Inert gas temperature	25-200 °C	25 °C
Feed chemical composition	Various feedstocks	-

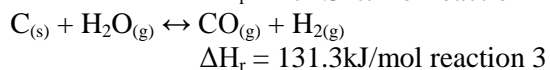
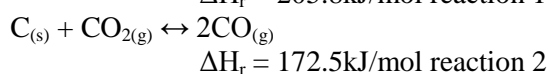
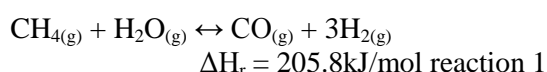
Table 4: values of the operating variables in terms of ranges and increments.

3 Problem Solution

The main components of the gaseous product resulting from the simulated pyrolysis, besides nitrogen coming from the inert carrier gas, are molecular hydrogen (H₂), carbon monoxide (CO), carbon dioxide (CO₂) and methane (CH₄), while the remainder comprises mostly water (H₂O) and little amounts of heavier alkanes and alkenes. Figure 3 reports the trend of the pyrolysis gas composition (mole fractions, without N₂) with temperature of these five leading species.

From this graph it is readily seen how the amounts of H₂ and CO increase with temperature and that the opposite trend is observed for the quantities of CO₂, CH₄ and H₂O. This is the trend found and confirmed during several pyrolysis and gasification experiments of biomass [25,27].

The following well-known reactions can explain the trends seen exhibited in figure 3:



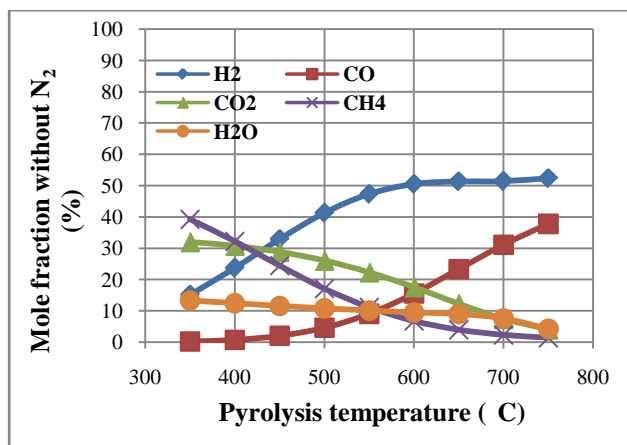


Fig.1: mole fractions of H₂, CO, CO₂, CH₄ and H₂O in the gas product as functions of pyrolysis temperature.

The first one, i.e., the “steam reforming” reaction [28], starting from methane and water, yields carbon monoxide and molecular hydrogen. The second reaction, i.e., the “Boudouard’s equilibrium” [29], describes the equilibrium between CO and CO₂ in presence of graphitic carbon. The last equation is known as “heterogeneous water gas reaction” [30]. Particularly, they are all endothermic reactions and so they are favored by higher temperatures; they consume CH₄, CO₂ and H₂O to give CO and H₂.

The graphitic carbon, which is obviously in the char, is consumed according to reactions 2 and 3; then, it is interesting to discuss the issue of the char carbon mass fraction in the pyrolysis reactor, which has been predicted by assuming that pyrolyzed solids are constituted of ashes and the carbon residue only.

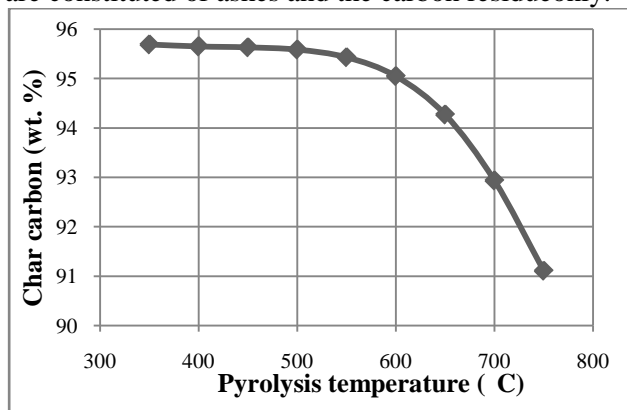
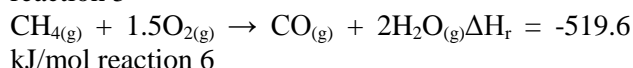
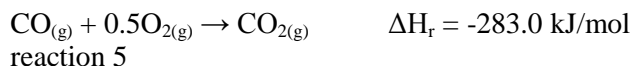
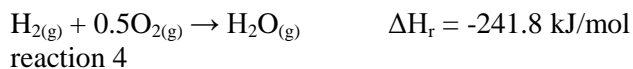


Fig. 4: char carbon mass fraction as a function of pyrolysis temperature.

In figure 4 the trend of char carbon mass fraction against the pyrolysis temperature is depicted. As expected, this figure illustrates that the carbon content decreases with temperature. The important thing to notice is that, like for CO₂, the decrease of the char carbon is larger at higher temperatures, thus demonstrating that the Boudouard equilibrium taken into account by the model is becoming relevant.

As a matter of fact, one has to remember that, even if it is present in small amount, oxygen is another component of the reacting mixture and therefore there are also oxidation reactions to be considered. The main oxidation reactions occurring within the pyrolysis gas mixture are the following:

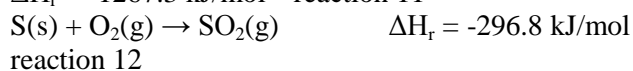
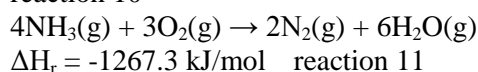
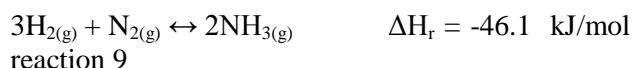


Since these are all oxidation reactions they are also exothermic and non-equilibrium reactions; anyway, reactions 7 and 8 are heterogeneous and they can be slowed down by mass transport resistances that the oxygen must overcome to come into contact with the solid carbon. The most likely pattern is that the oxidation reactions are fast enough to precede the endothermic equilibrium ones such that to consume all of the available oxygen.

The importance of the oxidation reactions grows with the oxygen content in the carrier gas; they are enhanced also by non-bounded molecular oxygen within the biomass feedstock itself. Nevertheless, for a usual pyrolysis process with proper inert carrier gas, they are of minor importance.

The possible formation of pollutants has been considered as well, and, among the many, the possible pollutants considered in the model are nitrogen monoxide (NO), nitrogen dioxide (NO₂), ammonia (NH₃), sulfur dioxide (SO₂), sulfur trioxide (SO₃) and hydrogen sulfide (H₂S). However, within the results of the simulation, appreciable quantities have been found only for NH₃, H₂S and SO₂ whereas the other pollutants quantities are negligible.

Among the many possible reactions that can lead to these polluting species, the most important are:



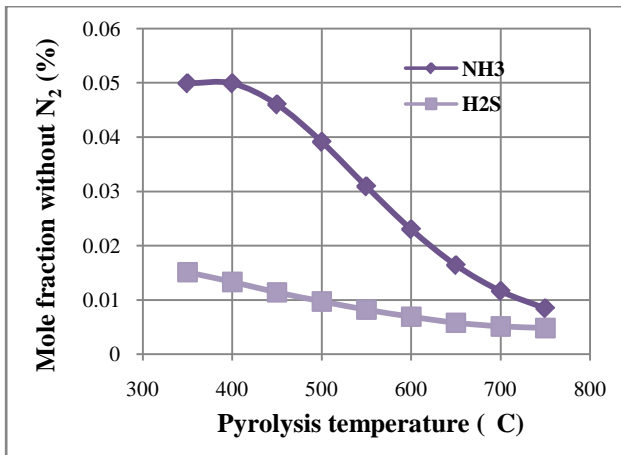


Fig. 5: NH₃ and H₂S mole fractions in the gas product as functions of pyrolysis temperature.

Figure 5 reports the trends of NH₃ and H₂S mole fractions while figure 6 reports the trend of SO₂ mole fraction as functions of pyrolysis temperature. These two figures show that the mole fractions of NH₃ and H₂S are quite small, less than 0.05%, and that SO₂ mole fraction is about nine orders of magnitude lower; nevertheless, it is still interesting to look at their trends. It can be seen that NH₃ and H₂S mole fractions decrease with temperature and the opposite behavior is exhibited by SO₂ as a consequence of equilibrium.

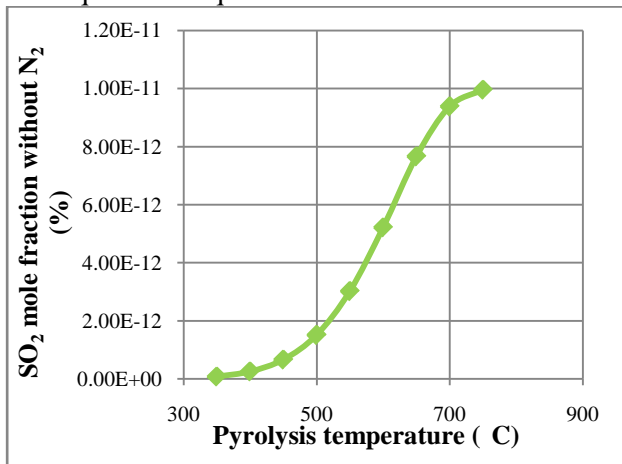


Fig. 6: SO₂ mole fraction in the gas product as a function of pyrolysis temperature.

A very important parameter characterizing the energetic level of a charcoal is the higher heating value (HHV). It represents the total heat released in MJ/kg or kJ/kg when the particular fuel is burnt considering the resulting water in the liquid phase. In literature, a number of equations can be found for an approximate estimation of the heating values of different carbon-based materials, especially coals. The majority of these equations are based on the ultimate analysis [31]; less work had been reported with regard to lignocellulosic materials, although

some equations have been proposed to estimate heating values from proximate and chemical analysis [32,33,34].

In order to estimate the higher heating value of the char obtained from the simulations, it has been chosen to utilize the equation developed by Cordero et al. [34], which is:

$$HHV = 354.3 FC + 170.8 VM \text{ kJ/kg} \quad \text{equation 1}$$

where FC is the fixed carbon in wt. % d.b. and VM is the volatile matter in wt. % d.b. of charcoal.

The trend of the char HHV with pyrolysis temperature, shown in figure 7, is similar to the one exhibited by the char carbon mass fraction because the above equation 1 is linear against it.

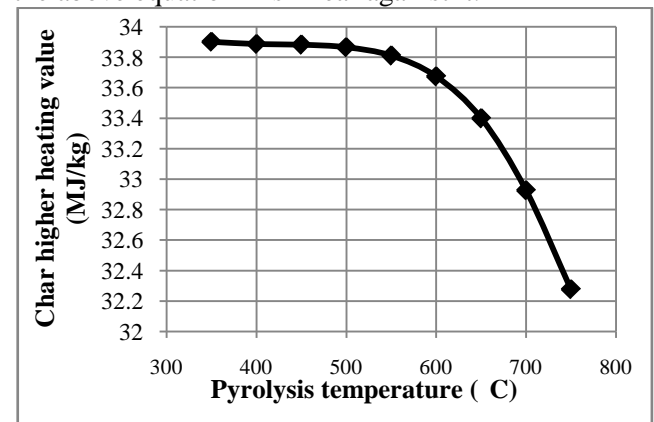


Fig.7: char higher heating value as a function of pyrolysis temperature.

As the gas composition is affected by temperature, this also significantly affects the Lower Heating Value of the gas product. The best way to get a LHV value as high as possible is to produce a gas enriched in CO, H₂ and CH₄, which could be suitable for energetic exploitation, for example in internal combustion engines and turbines for power production. The gas LHV has been calculated using equation 2, here reported [35]:

$$LHV = (30 * X_{CO} + 25.7 * X_{H_2} + 85.4 * X_{CH_4}) * 4.2 \text{ kJ/Nm}^3 \quad \text{equation 2}$$

where X_{CO} , X_{H_2} and X_{CH_4} are the mole fractions (as calculated considering N₂ while excluding H₂O) of CO, H₂ and CH₄, respectively.

Figure 8 shows the plot of the gas lower heating value (LHV) against pyrolysis temperature. The minimum reported for the LHV is obviously related to the previously discussed trends of CH₄, H₂ and CO. The concentration of methane, whose coefficient within equation 2 is the largest, decreases with temperature; this reduction is not

matched by the increase of H₂ and CO and so the net effect is that of lowering LHV down to 550°C. Above this latter T, the increase of H₂ and CO concentrations is such that LHV increases up to a maximum value of 8337 kJ/Nm³ at 750°C.

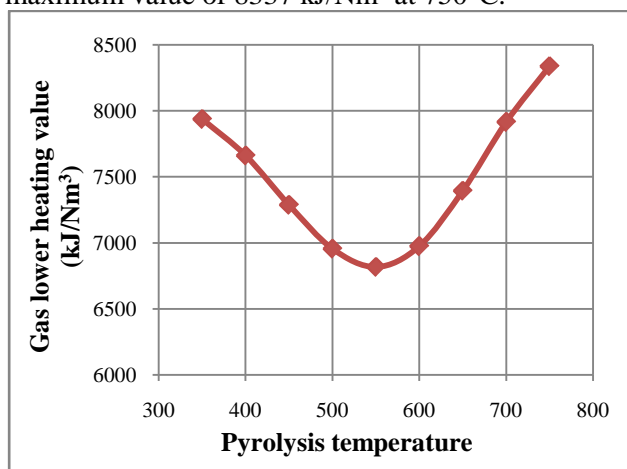


Fig. 8: gas lower heating value as a function of pyrolysis temperature.

As the pyrolysis reactor works at equilibrium, it has no dimensions; in particular, the heat transfer area cannot be evaluated and then the heat duty is evaluated just through an energy balance carried out by Aspen Plus[®]. Figure 9 displays the plot of the reactor net heat duty against pyrolysis temperature and, as expected, an increasing trend is found.

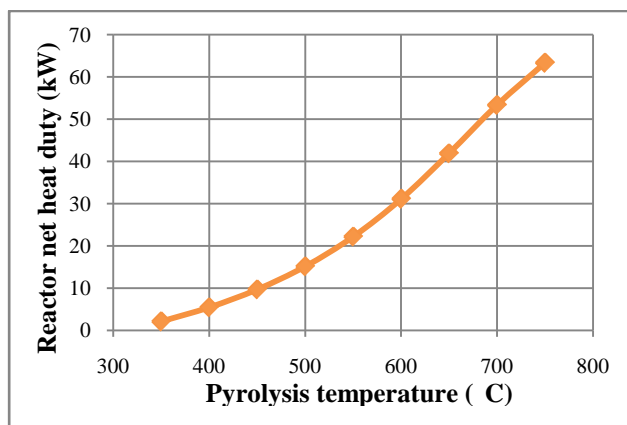


Fig. 9: reactor net heat duty as a function of pyrolysis temperature.

Considering the huge amount of results that the simulation is generating when the value of each operating variable is changed, it has been chosen to summarize the results here by means of trend tables. Therefore, table 4, 5, 6, 7 and 8 report the trends as a function of the process variables for the relative yields of char, tar and gas, the mole fractions of CO, CO₂, H₂, H₂O and CH₄ in the gas, the char carbon mass fraction, the pollutants mole fractions in the gas, the char higher heating value (HHV), the gas

lower heating value (LHV) and the net heat duty (NHD) required at the pyrolysis reactor, respectively.

	T	P	Inert gas O ₂ content	Inert gas flow rate	Inert gas T	Feed flow rate
Gas	↑	↓	↓	↑	-	↓
Liquid	↓	↑	↑	↓	-	↑
Char	↓	↓	↓	↓	-	↓

Table 4: effects of each process variable on char, liquid and gas relative amounts.

	T	P	Inert gas O ₂ content	Inert gas flow rate	Inert gas T	Feed flow rate
H ₂	↑	↓	↓	↑	-	↑↓
CO	↑	↓	↑	↑	-	↓
CO ₂	↓	↑	↑	↓	-	↑
CH ₄	↓	↑	↓	↓	-	↑
H ₂ O	↓	↑	↓	↑	-	↓

Table 5: effects of each process variable on the mole fractions of H₂, CO, CO₂, CH₄ and H₂O in the gas.

	T	P	Inert gas O ₂ content	Inert gas flow rate	Inert gas T	Feed flow rate
Char carbon mass fraction	↓	↓	↓	↑↓	-	↑

Table 6: effects of each process variable on char carbon mass fraction.

	T	P	Inert gas O ₂ content	Inert gas flow rate	Inert gas T	Feed flow rate
NH ₃	↓	↑	↓	↑	-	↑↓
H ₂ S	↓	↑	↓	↓	-	↑
SO ₂	↑	↑	↑	↓	-	↑

Table 7: effects of each process variable on the mole fractions of NH₃, H₂S and SO₂ in the gas.

	T	P	Inert gas O ₂ content	Inert gas flow rate	Inert gas T	Feed flow rate
Char HHV	↓	↓	↓	↑↓	-	↑
Gas LHV	↓↑	↑	↓	↓	-	↑
Reactor NHD	↑	↓	↓	↑	↓	↑

Table 8: effects of each process variable on char HHV, gas LHV and reactor NHD.

Taking advantage of the Aspen[®] capabilities, the trend analysis has been further extended to consider a possible variation in the feedstock, e.g., to brown coal and waste tyres, whose compositions have been reported in Tables 1 and 2 as well. The values of the main predicted simulation results are in Tables 9, 10, 11, 12 and 13.

	Volatile matter	Ash content	O content
	52.51-70.86-84.71	1.35-5.7-6.11	0.01-24.58-43.98
Gas	62.4-51.65-71	71-62.4-51.65	51.7-62.4-71
Liquid	8.14-0.06-11.42	11.4-8.1-0.06	0.06-8.1-11.4
Char	29.5-48.3-17.61	17.61-29.5-48	48-29.5-17.6

Table 9: effects of some components of the ultimate and proximate analyzes on % yieldsof gas, liquid and char.

	C content	O content	Moisture content
	47.67-63.51-85.4	0.01-24.58-43.98	1.71-7.86-13.56
H ₂	41.3-44.2-56.9	56.9-44.2-41.3	56.9-41.3-44.2
CO	4.64-4.31-0.29	0.29-4.31-4.64	0.29-4.64-4.31
CO ₂	26.1-21.1-0.12	0.12-21.1-26.1	0.12-26.1-21.1
CH ₄	17.1-18.4-37.7	37.7-18.4-17.1	37.7-17.1-18.4
H ₂ O	10.8-11.9-4.5	4.5-11.9-10.8	4.5-10.8-11.9

Table 10: effects of some components of the ultimate and proximate analyzes on the % mole fractions of H₂, CO, CO₂, CH₄ and H₂O in the gas.

	Ash content	O content	Volatile matter
	1.35-5.7-6.11	0.01-24.58-43.98	52.51-70.86-84.71
Char carbon mass fraction	95.6-89.6-92.2	92.2-89.6-95.6	89.6-92.2-95.6

Table 11: effects of some components of the ultimate and proximate analyzes on % mass fractionof char carbon.

	S content	N content	C content	O content
	0.01-0.06-0.44	0.13-0.48-1.01	47.67-63.51-85.4	0.01-24.58-43.98
NH ₃	0.039-0.046-0.084	0.039-0.084-0.046	0.039-0.046-0.084	0.084-0.046-0.039
H ₂ S	0.0097-0.067-0.5	0.0097-0.5-0.067	0.0097-0.067-0.5	0.5-0.067-0.0097
SO ₂	1.51*10 ⁻¹² -7.9*10 ⁻¹² -2.51*10 ⁻¹³	1.51*10 ⁻¹² -2.51*10 ⁻¹³ -7.9*10 ⁻¹²	1.5*10 ⁻¹² -7.9*10 ⁻¹² -2.51*10 ⁻¹³	2.5*10 ⁻¹³ -7.9*10 ⁻¹² -1.51*10 ⁻¹²

Table 12: effects of some components of the ultimate analysis on the % mole fractions of NH₃, H₂S and SO₂ in the gas.

	Ash content	O content	C content	Volatile matter	Moisture content
	1.35-5.7-6.11	0.01-24.58-44	47.7-63.5-85.4	52.5-70.9-84.7	1.7-7.9-13.6
Char HHV (MJ/kg)	33.9-31.7-32.7	32.7-31.7-33.9	33.9-31.7-32.7	31.7-32.7-33.9	32.7-33.9-31.7
Gas LHV (kJ/Nm ³)	6955-6709-11379	11379-6709-6955	6955-6709-11379	6709-11379-6955	11379-6955-6709
Reactor NHD (kW)	15.2-12.4-12.9	12.9-12.4-15.2	15.2-12.4-12.9	12.4-12.9-15.2	12.9-15.2-12.4

Table 13: effects of some components of the ultimate and proximate analyzes on char HHV, gas LHV and reactor NHD.

It is very interesting to compare some of these results with those obtained through experiments by Honus [25]. Particularly, the composition and volumetric flow rate of the pyrolysis gas stream have been re-calculated by using the Aspen simulation code and by correspondingly changing the feedstock composition; then, the predicted values have been compared to those found by Honus in tables 14 and 15, respectively.

	T (°C)	Mole fractions without inert gas N ₂ (%)							
		Predicted				Experimental			
		H ₂	CO	CO ₂	CH ₄	H ₂	CO	CO ₂	CH ₄
Biomass	500	40.4	4.29	27.4	20.0	6.4	8.7	20.3	16.4
	550	47.0	8.47	23.6	13.3	13.2	8.0	19.9	14.9
	600	50.8	14.7	18.8	8.25	18.7	12	18.3	15.4
	650	52.1	22.4	13.4	4.87	19.9	31	16.2	15.1
Brown coal	500	43.1	3.92	22.2	22.2	15.1	11	19.2	25.3
	550	50.1	7.78	19.3	14.7	19.5	10	18.3	20.7
	600	54.1	13.5	15.5	9.07	27	11	18.1	24.4
	650	55.4	20.6	11.0	5.35	33.9	12	16.1	14.8
Waste tyres	500	51.8	0.19	0.07	43.5	12.4	2.8	2.4	27.9
	550	65.1	0.45	0.08	30.7	13.3	3.7	2.3	19.8
	600	75.9	0.89	0.08	20.2	22.2	3.1	1.9	19.2
	650	83.6	1.47	0.06	12.8	28.3	3.9	1.4	4.6

Table 14: experimental and predicted % mole fractions of H₂, CO, CO₂ and CH₄ at different pyrolysis temperatures from different feedstocks.

The first observation derived from table 14 is that the predicted mole fractions, especially those of H₂, are sometimes far from the experimental ones: this is not surprising here because the assumption of chemical equilibrium in this work is a very strong one. Actually, the duration of Honus' batch experiments was about 45 minutes and, even if his process can be classified as slow pyrolysis or "gasification pyrolysis", it is still not enough to approach the chemical equilibrium. However, even if the predicted and experimental values are far from each other, the general trends as a function of the operating variables are satisfactory meaning that the predicted values are the ones to which the experimental ones try to tend.

	T (°C)	Volumetric flow rate (m ³ /s)	
		Predicted	Experimental
Biomass	500	0.006	0.00237
	550	0.00714	0.00281
	600	0.00853	0.00313
	650	0.01012	0.00352
Brown coal	500	0.00482	0.0009
	550	0.00571	0.00142
	600	0.0068	0.00145
	650	0.00803	0.00203
Waste tyres	500	0.0058	0.00178
	550	0.00638	0.00219
	600	0.00695	0.00202
	650	0.00745	0.0028

Table 15: experimental and predicted volumetric gas flow rate at different pyrolysis temperatures from different feedstocks.

The predicted values of the volumetric gas flow rate are of the same order of magnitude of the experimental ones, but still about 2-3 times higher, as it is reported in table 15. This is again due to the assumption of chemical equilibrium, which can be approached and seldom achieved where all the volatile matter is released. Also in this case, the predicted trends as a function of the pyrolysis temperature agree with what is experimentally seen, as for the trends of the gaseous species.

4 Conclusion

The main limiting assumption of the model developed in this work is that the residence time is considered to be long enough and the reaction rates are supposed to be fast enough to reach thermodynamic equilibrium. The comparison made of the predicted results with some experimental ones just taken as a reference has proved that even a residence time of 45 min is not enough to achieve thermodynamic equilibrium, but hours or days could be required. Unfortunately, performing pyrolysis processes with so long residence of the feed and the inert carrier gas is too energy-demanding and out of practical interest. On the other hand, thermodynamic equilibrium calculations have the advantage of being independent of the flow pattern and so of the specific pyrolysis reactor design. This leads to the fact that this approach – and therefore the present Aspen simulation model – is very versatile and can be applied for all pyrolysis systems; so, it can be used to study only the effect of the process variables while it cannot give accurate predictions of the desired process quantities.

Possible solutions to improve the accuracy of equilibrium-based models could be that of modifying or correcting the equilibrium model through the use of experimental results or developing models based on quasi-equilibrium temperature approaches; in fact, these have proved to give acceptable results when applied to biomass gasification [36,37].

Kinetic models are opposed to equilibrium models in that they describe the conversion during biomass pyrolysis, which is crucial in designing, evaluating and improving pyrolysis systems; so, they need kinetic rate expressions obtained from experiments. These rate models, unlike equilibrium models, are accurate and detailed but are computationally intensive and their applicability is limited to the pyrolysis system from which the experimental kinetic information have been found.

From these considerations it is clear that the development of a universal mathematical model,

capable of predicting with a good accuracy the products of a pyrolysis process of whatever feedstock in every reactor configuration, should combine the versatility of equilibrium models and the accuracy of kinetic models; this is a challenge to develop proper design procedures for pyrolysis systems. Once done, the potential of biomass as a renewable source can be further exploited all over the world to relieve the burden of the energy supply of fossil fuels and meanwhile to ease the environmental problem.

References:

- [1] United Nations Environment Programme. Renewable energy: investing in energy and resource efficiency http://www.unep.org/greeneconomy/Portals/88/documents/ger/GER_6_RenewableEnergy.pdf; (2011).
- [2] Griu T., Lunguleasa A. Exotic and Native Species as Biomass for Renewable Energy. *Advances in Environmental Technology and Biotechnology*, 2014, ISBN:978-960-474-384-1.
- [3] Messerle V. E., Ustimenko A. B., Lavrichshev O. A. Plasma Gasification of Solid Fuels. *Recent Advances in Energy, Environment and Economic Development*, 2012, ISBN: 978-1-61804-139-5.
- [4] Riehl R. R., Shahateet C. A., De Souza L. S., Dib Karam Jr. Biomass Gasification Unit Using Sugar Cane Bagasse for Power Generation. *Recent Advances in Energy, Environment and Economic Development*, 2012, ISBN: 978-1-61804-139-5.
- [5] Miccio M. and Cosenza B., Fuzzy Control of a Biomass-Fired and Solar-Powered Fluidized Bed Prototype as a Residential Cogeneration System, Proceedings (with peer review) of the 3rd Int. Conf. on Energy Systems, Environment, Entrepreneurship and Innovation (ICESEEI '14), ISSN: 2227-4359, ISBN: 978-960-474-375-9, Salerno, 17-26, June 3-5, 2014
- [6] Mohan D., Pittman C. U., Steele P. H. Pyrolysis of wood/biomass for bio-oil: a critical review. *Energy & Fuels*, Vol.20, 2006, pp. 848-89.
- [7] Prins W., Wagenaar B. M. Review of rotating cone technology for flash pyrolysis of biomass. In: *Kaltschmitt M. K., Bridgwater A. V., editors. Biomass gasification and pyrolysis*. UK: CPL Scientific Ltd.; 1997. p. 316-26.
- [8] Peacocke G. V. C., Bridgwater A. V. Ablative plate pyrolysis of biomass for liquids. *Biomass Bioenergy*, Vol.7, 1995, pp. 147-54.
- [9] Heinrich E., Dahmen N., Dinjus E. Cost

- estimate for biosynfuel production via biosyncrude gasification. *Biofuels BioprodBioref*, Vol.3, 2009, pp. 28-41.
- [10] Wu C., Wang Z., Huang J., Williams P. T. Pyrolysis/gasification of cellulose, hemicellulose and lignin for hydrogen production in the presence of various nickel-based catalysts. *Fuel*, Vol.106, 2013, pp. 697-706.
- [11] J. J. M. Orfao, F. J. A. Antunes, J. L. Figuereido. Pyrolysis kinetics of lignocellulosic materials-three independent reactions model. *Fuel*, Vol.78, 1999, pp. 349-358.
- [12] Raveendram K., Ganesh A., KhilarK.C. Pyrolysis characteristics of biomass and biomass components. *Fuel*, Vol.75, 1996, pp. 987-98.
- [13] H. Yang, R. Yan, H. Chen, C. Zheng, D. Lee. In-depth investigation of biomass pyrolysis based on three major components: hemicellulose, cellulose and lignin. *Energ. Fuel*, Vol.20, 2006, pp. 388-393.
- [14] N. Worasuwanarak, T. Sonobe, W. Tanthapanichakoon. Pyrolysis behaviors of rice straw, husk and corncob by TG-MS technique. *J. Anal. Appl. Pyrol.*, Vol.78, 2007, pp. 265-271.
- [15] G. Wang, W. Li, B. Li, H. Chen. TG study on pyrolysis of biomass and its three components under syngas. *Fuel*, Vol.87, 2008, pp. 552-558.
- [16] S. Wang, X. Guo, K. Wang, Z. Luo. Influence of the interaction of components on the pyrolysis behavior of biomass. *J. Anal. Appl. Pyrol.*, Vol.91, 2011, pp. 183-189.
- [17] Ranzi E., Cuoci A., Faravelli T., Frassoldati A., Migliavacca G., Pierucci S., Sommariva S. Chemical Kinetics of Biomass Pyrolysis. Department Politecnico di Milano, Milano, Italy. *Energy & Fuels*, Vol.22, 2008, pp. 4292-4300.
- [18] Piskorz J., Radlein D., Scott D. S. On the mechanism of the rapid pyrolysis of cellulose. *J. Anal. Appl. Pyrol.*, Vol.9, 1986, pp. 121-37.
- [19] Banyasz J. L., Li S., Lyons-Hart J. L., Shafer K. H. Cellulose pyrolysis: The kinetics of hydroxyacetaldehyde evolution. *J. Anal. Appl. Pyrol.*, Vol.57, No.2, 2001, pp. 223-248.
- [20] Banyasz J. L., Li S., Lyons-Hart J. L., Shafer K. H. Gas evolution and the mechanism of cellulose pyrolysis. *Fuel*, Vol.80, No.12, 2001, pp. 1757-1763.
- [21] Suuberg E. M., Milosavljevic I., Vahur O. *Proc. Comb. Institute*, Vol.26, 1996, pp. 1515.
- [22] Faravelli T., Frassoldati A., Ranzi E., Hugony F., Migliavacca G. Modellazione dettagliata della pirolisi di biomasse: Modelli cinetici di devolatilizzazione. *La RivistadeiCombustibili*, Vol.61, No.5, 2007, pp. 249-270.
- [23] Aspen Tech Corporate Overview http://www.aspentech.com/corporate/press/media_kit.aspx.
- [24] Lantagne G., Marcos B., Cayrol B. Computation of complex equilibria nonlinear optimization. *Comput.Chem. Eng.*, Vol.12, No.6, 1988, pp. 589-599.
- [25] Honus S. Gaseous components from pyrolysis – characteristics, production and potential for energy utilization. ISSN 1330-3651 (print), ISSN 1848-6339 (Online) UDC/UDK.
- [26] Peng D.-Y., Robinson D. B., A New Two-Constant Equation-of-state. *Ind. Eng. Chem. Fundam.*, Vol.15, 1976, pp. 59-64.
- [27] DufourA., Girods P., Masson E., Rogaume Y., Zoulalian A. Synthesis gas production by biomass pyrolysis: effect of reactor temperature on product distribution. *International journal of hydrogen energy*, Vol.34, 2009, pp. 1726-1734.
- [28] http://en.wikipedia.org/wiki/Steam_reforming
- [29] http://en.wikipedia.org/wiki/Boudouard_reaction
- [30] http://en.wikipedia.org/wiki/Water_gas.
- [31] Francis H. E., Lloyd W. G. *J. Coal Qual.*, Vol.2, No.2, 1983, pp. 21.
- [32] Jimenez L., Gonzalez F. *Fuel*, Vol.70, No.8, 1991, pp. 947.
- [33] Shafizadeh F., Degroot W. G. Thermal uses and properties of carbohydrates and lignins. *New York: Academic Press*, 1976.
- [34] Cordero T., Marquez F., Rodriguez-Mirasol J., Rodriguez J.J. Predicting heating values of lignocellulosics and carbonaceous materials from proximate analysis. *Fuel*, Vol.80, 2001, pp. 1567-1571.
- [35] Lv P.M., XiongZ.H., Chang J., Wu C.Z., Chen Y., Zhu J.X. An experimental study on biomass air-steam gasification in a fluidized bed. *Bioresource Technology*, Vol.95, 2004, pp. 95-101.
- [36] Zainal Z. A., Ali R., Lean C. H., Seetharamu K. N. Prediction of performance of a downdraft gasifier using equilibrium modelling for different biomass materials. *Energy Convers. Manage*, Vol.42, 2001, pp. 1499-155.
- [37] Jarugthammachote S., Dutta A. Equilibrium modeling of gasification: Gibbs free energy minimisation approach and its application to spouted bed and spout-fluid bed gasifiers. *Energy Convers. Manage*, Vol.49, 2008, pp. 1345-1356.